Circular gratings recorded as axicon interferograms

BOŻENA JANOWSKA-DMOCH

Warsaw University, ul. Pasteura 1, 02–093 Warszawa, Poland.

BOHDAN MROZIEWICZ

Institute of Electron Technology, al Lotników 32/46, 02–668 Warszawa, Poland.

Circular diffraction gratings have recently found interesting applications in photonics, particularly, in technology of semiconductor surface emitting lasers. Efficient methods of producing such gratings on semiconductor surface are therefore sought. In the paper, circular gratings recorded by conic-wave-front interefrence are presented and their properties described. The axicon waves have been produced both by transmission of the laser beam through a glass cone and by its reflection from a conic mirror.

1. Introduction

Diffraction gratings have been used in a variety of applications such as distributed feedback (DFB) and distributed Bragg reflector (DBR) lasers [1], mode order converters [2], light wave couplers [3], band rejection filters [4] and electrooptic deflectors [5]. Gratings used in these devices typically consist of a set of parallel, uniformly spaced straight lines. However, a special class of gratings with circular symmetry has recently attracted particular attention. Such gratings can serve as diffractive axicons and used either in transmission [6] or reflection [7] modes to generate, in good approximation, a non-diffracting Bessel beam [8]. It is well known that such a beam propagates in free space with the energy confined to its axis and theoretically does not experience any spreading or divergence [9]. In practice, the finite aperture of the experimental elements used to generate circular gratings causes that the beam is only an approximation to a Bessel function and that restricts the available non-spreading range.

Several alternative means of generating circular gratings have been suggested, including an electron-beam [10]−[13] or ion-beam lithography [14]−[16], inter-ferometric methods [17] and the methods based on the computer generated binary phase holographic optical elements (HOE), [18], [19]. For most applications the grating constant ought to be only a small fraction of micrometer, at the same time very high quality of the grating is necessary to couple circular modes. Even small nonuniformities, like variations in depth of its grooves with regard to its period of the order of 1%, have a significant effect on the power in the output beam of the DBR structures [11], [20]. This sets very strong quality requirements on the

method used to produce the grating on the laser surface. The lithographic methods are advantageous in the case of narrow-pitched and free-shaped patterns, but the range of the practical grating dimensions is restricted to diameters below 1 mm and the process of writing is time consuming. That makes these methods rather unsuitable for mass production. In the effort to overcome this difficulty we have investigated in the present work optical interference methods following the idea proposed by Leith *et al.* in 1990 [21]. According to this idea, a circular grating may be formed as a result of interference of the light waves, one of which is conic. The interference pattern can be then restricted in a photosensitive material in the form of an interferogram.

Circular gratings recorded by conic-wave-front interference are presented here and their properties studied. The axicon waves have been produced either by transmission of the laser beam through a transparent cone or by its reflection from a conic mirror.

2. Interferograms of a transparent cone

The experimental set-up used to generate and record circular fringes formed with the aid of a transparent cone is shown in Fig. 1. The expanded, filtered and collimated beam from He-Ne laser was used to illuminate a glass cone with the cone angle $\Theta = 16°$. The incident light beam was parallel to the cone axis and illuminated the cone from its apex side. The photosensitive material (RM) was placed behind the cone in the region where the incident plane wave takes on the shape of conic waves with the same obtuse angle equal to Θ. Apices of the forming light cones are located on a straight line and form a linear focus. The registering material is placed in this focus region of the interfering conic waves and a circular diffraction pattern is therefore created.
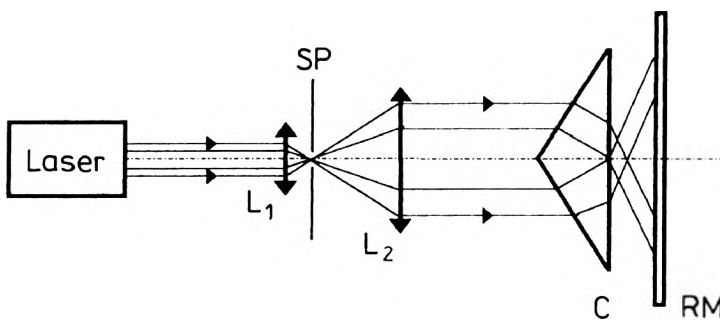
Fig. 1. Optical system used to record the glass cone interferograms. Lenses L_1, L_2 and spatial filter SP form a collimator expanding the laser beam that illuminates the glass cone C. Behind the cone there is located the recording material RM.

The electric field distribution $E(r, z)$ in the plane located at a distance z behind the cone (in paraxial approximation) is given by the Fresnel integral (see Fig. 2), [22]
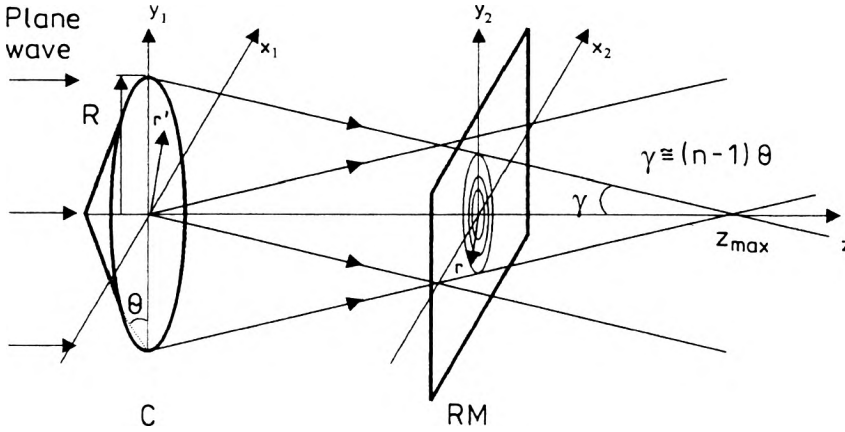
Fig. 2. Schematic diagram illustrating formation of a circular grating on the recording material RM when the plane light wave is pasing through the glass cone C. Here, R is the radius of the cone base, Θ is the cone angle, r' and r are the polar coordinates in the planes $(x_1, y_1, 0)$ and $(x_2, y_2, 0)$, respectively.

$$E(r,z) = -\frac{ik}{z} E_0 \exp\left[ik\left(z + \frac{r^2}{2z}\right)\right] \int_0^R F(r') \exp\left(\frac{ik}{2z} r'^2\right) J_0\left(\frac{kr}{z} r'\right) r'\, dr' \tag{1}$$

where: E_0 is an amplitude of the incident light, k is the absolute value of wave vector, $F(r)$ is transmission function of the cone with radius R, $J_0\left(\dfrac{kr}{z} r'\right)$ is the zero order Bessel function. If neglecting reflection and transmission losses, the function $F(r)$ takes the form

$$F(r) = \exp\left(-\frac{i\pi}{\Lambda} r\right) \tag{2}$$

where grating period Λ is related to the geometry of the cone by

$$\Lambda = \frac{\lambda}{2(n-1)\Theta}. \tag{3}$$

Here, n is the refractive index of the glass cone with the angle Θ. After inserion of the transmission function $F(r)$ as in (2), the Fresnel integral can be solved approximately with the stationary phase method [22] and the following result can be obtained for the light intensity

$$I(r,z) = \frac{2\pi}{k} I_0 \frac{\pi^2 z}{\Lambda^2} J_0^2\left(\frac{\pi}{\Lambda} r\right) \tag{4}$$

where I_0 is the intensity of the incident light.

The Fresnel diffraction pattern of a glass cone consists of circular bright and dark fringes. It can be recorded if the recording material is placed at a distance z within the range of $0 < z < z_{\max}$ with

$$z_{max} = \frac{2R}{\Theta}.$$

(5)

In our case the material used for recording was a high-resolution photographic plate Holotest 8E75 placed at a distance $z = 3$ mm, while $z_{max} = 160$ mm.

a

100 μm

b

100 m
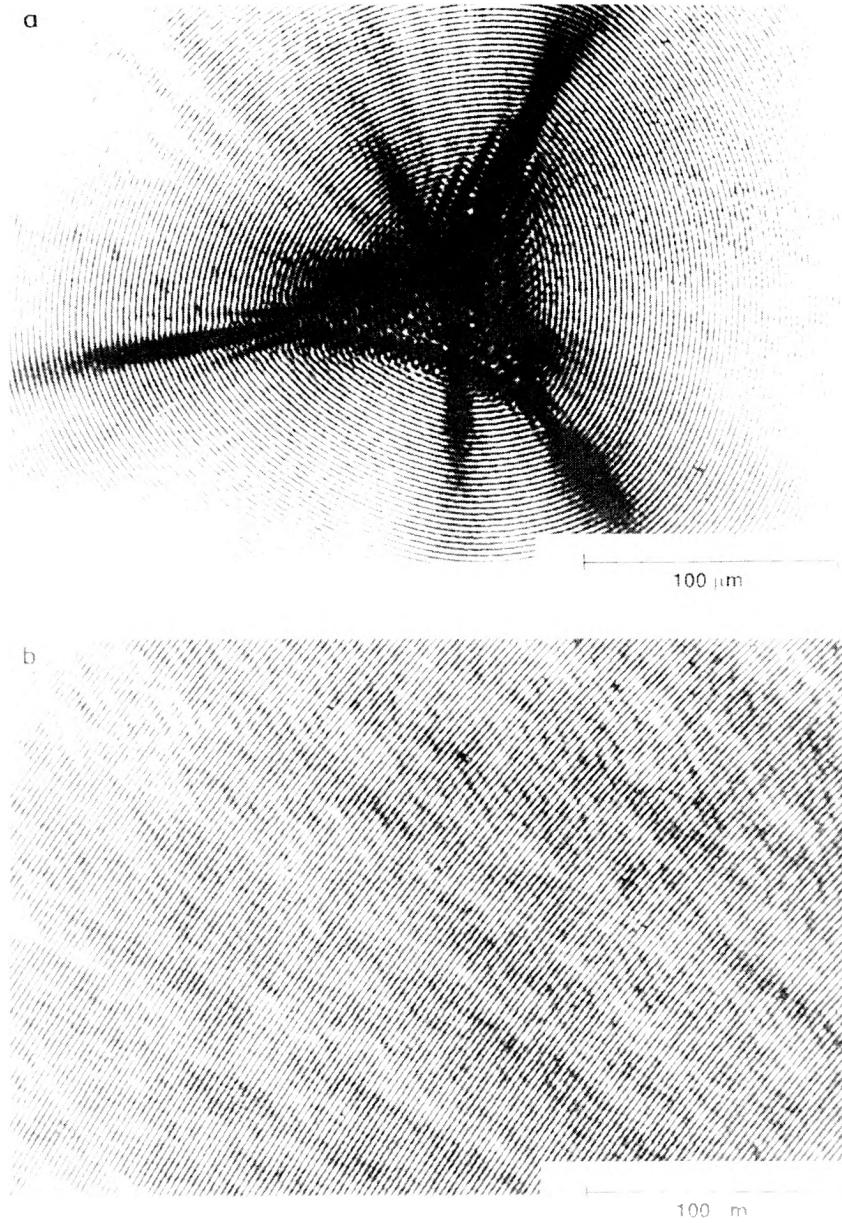
Fig. 3. Fringe pattern magnified 520 times: **a** — central part of the interferogram **b** — peripheral part of the pattern.

A photograph of the fringe pattern magnified 520 times is shown in Fig. 3. The grating period measured from the photographs is $\Lambda = 2.34 \pm 0.03$ μm, which within the limits of the approximation used is in agreement with the expected value. Radial spatial frequency of the grating $f_0 = \dfrac{1}{\Lambda} = 431$ line/mm and is constant in the whole fringe field (Fig. 3b). However, in the central part of the interference pattern (Fig. 3b) we can see that the shape of the fringes has no more circular symmetry and instead of a system of concentric rings we obtained fringes with the same spatial frequency, but looking like rounded up triangles. Such as shape is most probably caused by imperfections of the apex of the glass cone which generated aberrations in the optical system.

3. Diffraction properties of the recorded fringe pattern

The far field diffraction pattern of the grating illuminated by a plane wave is composed of the central zero-order beam and several concentric doubled rings. Such a splitting of diffraction rings may be explained if the function representing an arbitrary grating with circular symmetry and period Λ is expanded into a Fourier series [23]

$$f(r) = \sum_{-\infty}^{\infty} c_m \exp\left(-i\pi \frac{m}{\Lambda} r\right), \tag{6}$$

with the Fourier coefficients

$$c_m = \frac{1}{2\Lambda} \int_0^{2\Lambda} f(r) \exp\left(i\pi \frac{m}{\Lambda} r\right) dr. \tag{7}$$

The complex transmission function $T(r)$ of a grating can be written as

$$T(r) = c_0 + \sum_{m=1}^{\infty} c_m \exp\left(-i\frac{\pi m}{\Lambda} r\right) + \sum_{m=1}^{\infty} c_{-m} \exp\left(i\frac{\pi m}{\Lambda} r\right). \tag{8}$$

The first term c_0 is equivalent to undiffracted zero-order beam, the second and third terms describe conical convergent and divergent beams, respectively. These beams

a
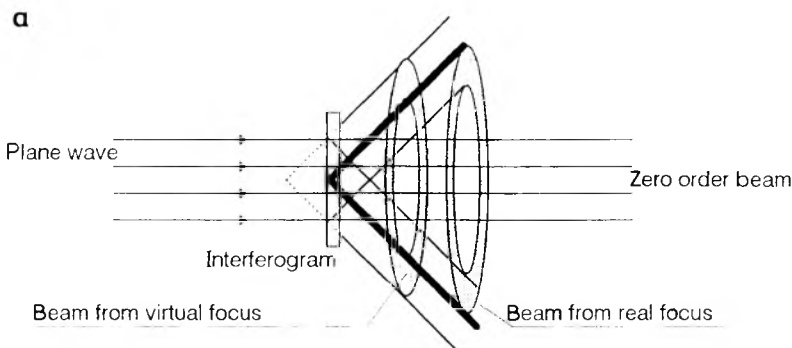
Fig. 4a
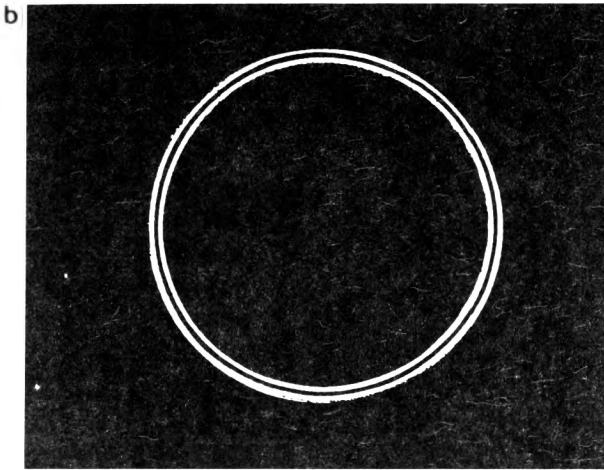
Fig. 4. Light diffraction on the interferogram of the cone; a — schematic representation of diffracted beams, b — far field diffraction pattern (the zeroth order diffraction beam has been screened).
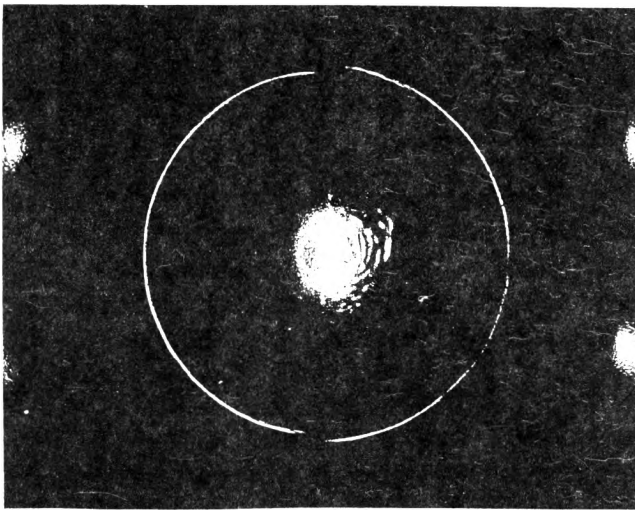
Fig. 5. Diffraction pattern of the glass cone interferogram with a knife-edge cut off half of the pattern.

are shown schematically in Fig. 4a. In Figure 4b, only the first order diffraction ring is shown, since the intensity of the rings decreases rapidly with increasing order m and the light field of higher order beams is too weak to be recorded. The same structure has been observed in higher order diffraction rings as well as in the first one, which can be explained as a result of destructive interference of conical convergent and divergent beams. The knife edge experiment (Fig. 5) shows that the beams forming the diffraction ring are conjugated one to another. It is possible to separate these beams using the lens with focal length $f = 50$ mm. Each part of the
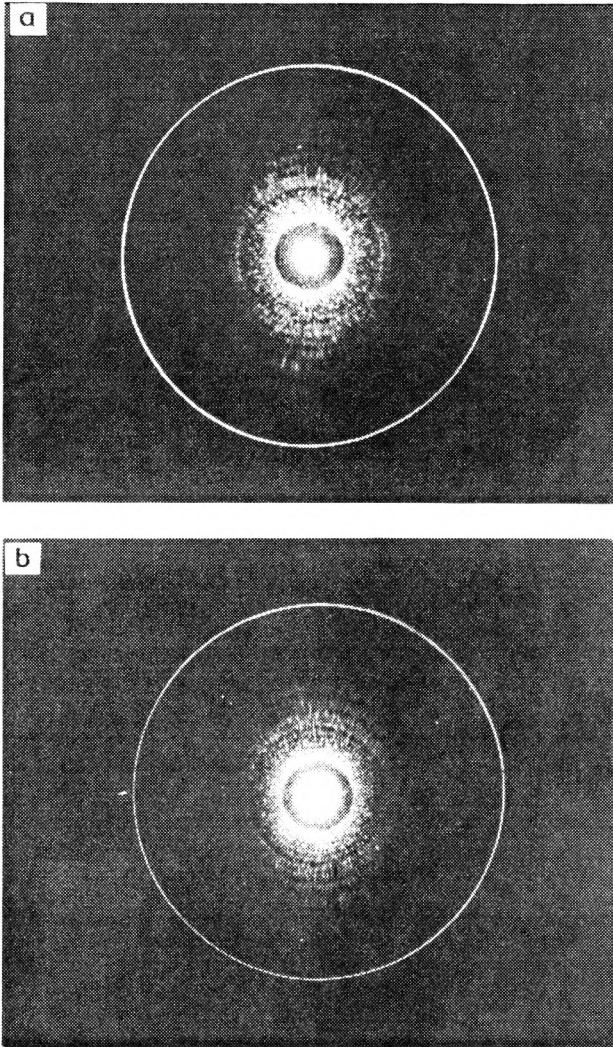
Fig. 6. Diffraction images obtained after using a lens: **a** — divergent beam-virtual focus, **b** — convergent beam-real focus.

diffraction pattern focuses in different plane (Fig. 6) forming just one, very fine ring, surrounding the zero-order component.

Thus, it has been proved that circular gratings can be easily produced on semiconductor wafers using an optical system with a glass cone. However, as one can see from the photographs in Fig. 3, the following difficulties can be anticipated:

— Distribution of the light intensity in the registered interferogram is not uniform and drops with the distance from the optical axis according to $1/r$. Inserting a reverse amplitude filter in the beam illuminating the axicon would allow equalisation of the intensities in the fringe field.

— Diffraction noise coming from the material point defects and inaccuracies in the polishing of the cone surface is superimposed on the fringes produced. This noise could be eliminated in the grating interferometer arrangement proposed by Leith *et al.* [21].

In conclusion, experiments clearly indicate that in order to obtain the axicon interferogram of the quality adequate for applications in semiconductor lasers the glass cone must be fabricated with the utmost precision. In addition, the cone should be made of a homogeneous material with high refractive index like YAG for which $n = 1.823$. In order to obtain $\Lambda = 0.25$ μm while using a He-Cd laser, the cone with $\Theta = 56°$ should be used.

4. Interferograms of a conic mirror

For recording an interferogram of a conic mirror, the experimental set-up shown in Fig. 7 was used. The laser beam that illuminates the conic mirror passes through the recording material RM. The beam reflected from the mirror is a Bessel beam and interferes with a plane incident wave. This results in a circular fringe pattern with the grating period equal to

$$\Lambda = \frac{\lambda}{\sin 2\Theta} \tag{9}$$

where λ is the wavelength of the light that illuminates the mirror, Θ is the cone angle.
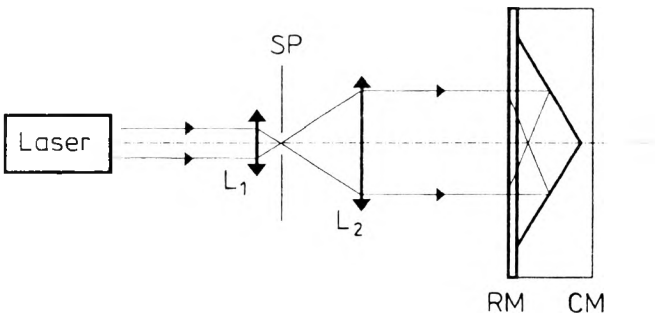
Fig. 7. Optical system used to register the conic mirror interferograms. Laser beam expanded by the collimator (lenses L_1, L_2 and the spatial filter SP) illuminates the conic mirror CM through the recording material RM.

The angle Θ in the mirror used in the experiments was $15°$ and therefore the obtained grating period was $\Lambda = 2\lambda$. Microscopic photographs from Fig. 8 show the conic mirror interferograms registered in the He-Ne light of the wavelength $\lambda = 0.633$ μm. Grating period found from the photographs is $\Lambda = 1.28$ μm and complies well within the experimental error limits with the expected value of $\Lambda = 1.27$ μm. The observed defects of the cone mirror interferogram are as follows:
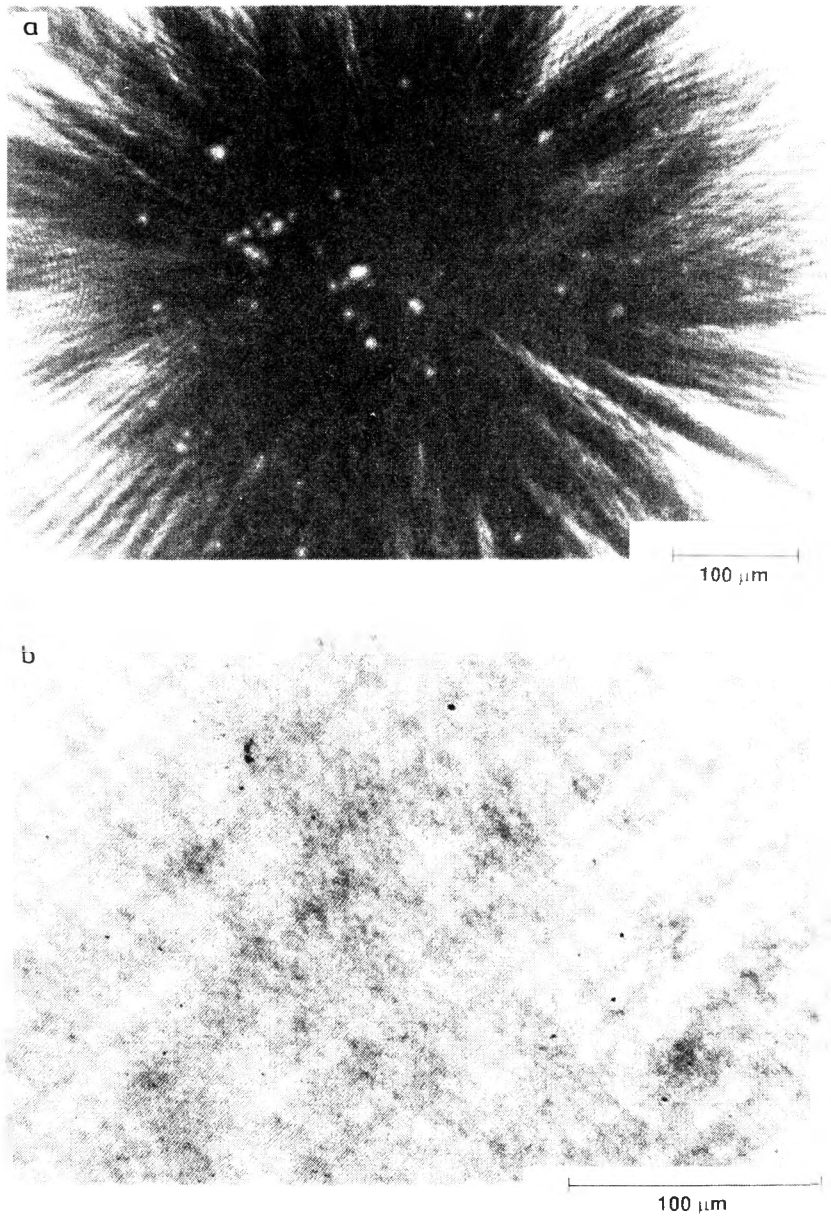
Fig. 8. Microscope photograph of a conic mirror interferogram: **a** — central part of the pattern magnified 260 times, **b** — peripheral part of the pattern magnified 520 times.

— High intensity distortions appear in the central part of the interferogram (Fig. 8a). They result from aberrations and surface defects of the mirror. Diameter of the area exceeds 500 μm.

— Light intensity distribution of the fringes registered on the recording material is non-uniform and drops as $1/r$ with the distance from the optical axis.

– Interference fringes are of low contrast. The effect is caused by interference of two beams with different intensity. It is because the incident beam interferes with a wave that is weakened by dispersion occurring while it passes through the registering material and then by reflection from the metallic surface.

5. Conclusions

The experiments described above have proved that although glass cone and cone mirror interferograms can be used for imprinting circular gratings, it is extremely difficult to obtain high quality gratings adequate to requirements imposed by the semiconductor laser technology.

References

[1] Mroziewicz B., Bugajski M., Nakwaski W., *Physics of Semiconductor Lasers*, PWN, North Holland, 1991.
[2] Zory P., Appl. Phys. Lett. **22** (1973), 125.
[3] Dakss M. L., Kuhn L., Heidrich P. F., Scott B. A., Appl. Phys. Lett. **16** (1970), 523.
[4] Schmidt R. V., Flanders D. C., Shank C. V., Standley R. D., Appl. Phys. Lett. **25** (1974), 651.
[5] Hammer J. M., Phillips W., Appl. Phys. Lett. **24** (1974), 545.
[6] Arimoto R., Saloma C., Tanaka T., Kawata S., Appl. Opt. **31** (1992), 6653.
[7] MacDonald R. P., Chrostowski J., Boothroyd S. A., Syrett B. A., Appl. Opt. **32** (1993), 6470.
[8] Durnin J., Miceli J. J., Eberly J. H., Phys. Rev. Lett. **58** (1987), 1499.
[9] Jiang Z., Lu Q., Liu Z., Appl. Opt. **34** (1995), 7183.
[10] Wu C., Svilans M., Fallahi M., Makino T., Glinski J., Maritan C., Blaauw C., Electron Lett. **27** (1991), 1819.
[11] Erdogan T., King O., Wicks G. W., Hall D. G., Dennis C. L., Rooks M. J., Appl. Phys. Lett. **60** (1992), 1773.
[12] Fallahi M., Dion M., Wasilewski Z., Buchanan M., Nournia M., Stapledon J., Barber R., Electron Lett. **31** (1995), 1581.
[13] Mroziewicz B., Dobrzański L., Electron. Technol. **30** (1997), 306.
[14] Wu C., Svilans M., Fallahi M., Templeton I., Makino T., Glinski J., Maciejko R., Najafi S. I., Maritan C., Blaauw C., Knight G., Electron. Lett. **28** (1992), 1037.
[15] Wu C. M., Svilans M., Fallahi M., Templeton I., Makino T., Glinski J., Maciejko R., Najafi S. I., Blaauw C., Maritan C., Knight D. G., IEEE Photon. Technol. Lett. **4** (1992), 960.
[16] Fallahi M., Chatenoud F., Templeton I. M., Dion M., Wu C. M., Delage A., Barber R., IEEE Photon. Technol. Lett. **4** (1992), 1087.
[17] Nishiwaki S., Asada J., Ohshima K., Kitagawa T., Appl. Opt. **34** (1995), 7372.
[18] Cox A. J., Dibble C., Appl. Opt. **30** (1991), 1330.
[19] Vasara A., Turunen J., Friberg A. T., J. Opt. Soc. Am. A **6** (1989), 1748.
[20] Mroziewicz B., Electron Technol. **32** (1999), No. 3, in print.
[21] Leith E., Chen H., Collins G., Scholten K., Swanson G., Upatnieks J., Appl. Opt. **19** (1980), 3626.
[22] Gori F., Guattari G., Padovani C., Opt. Commun. **64** (1987), 491.
[23] Niggl L., Lanzl T., Maier M., J. Opt. Soc. Am. A **14** (1997), 27.